2012 NDIA GROUND VEHICLE SYSTEMS ENGINEERING
AND TECHNOLOGY SYMPOSIUM
MODELING & SIMULATION, TESTING AND VALIDATION (MSTV) MINI-SYMPOSIUM
AUGUST 14-16 DEARBORN, MICHIGAN

MITIGATION OF OCCUPANT ACCELERATION IN A MINE-RESISTANT AMBUSH-PROTECTED VEHICLE BLAST EVENT USING AN OPTIMIZED DUAL-HULL APPROACH

Grant Schaffner, PhD
Adam Miller
University of Cincinnati
School of Aerospace Systems
Cincinnati, OH

ABSTRACT

With US military casualties mounting due to Improvised Explosive Devices (IEDs) and other roadside bombs, improving the protective capabilities of armored vehicles for service personnel is of paramount importance. Accurate numerical simulations of the blast event provide a means to quickly and economically evaluate the blast-protection performance of armored vehicles, and to develop improved blast countermeasures. This effort developed computational simulations of a system intended to mitigate blast accelerations to a level where the acceleration is no longer a lethal threat to the occupants of an armored vehicle. The hypothesis is that through the manipulation of the mass ratio, stiffness and damping properties of a dual-hull system, the capability of current Mine Resistant Ambush Protected (MRAP) vehicles can be greatly improved. The results show that, in comparison to the standard single-hull vehicle, the dual-hull vehicle reduces head injury criteria by 95.7%, neck compression by 78.3%, chest acceleration by 97.5% and leg forces by an average of 97%. Further work should focus on developing a realistic structural interface between the hulls and evaluating it using simulation, followed by fabrication and testing of limited test articles and full-vehicle systems.

INTRODUCTION

Improvised Explosive Devices (IEDs), along with other types of roadside bombs, have accounted for over 60% of American combat casualties in Iraq [1]. In Afghanistan, explosives account for 77% of field injuries and IEDs specifically account for 38% of all injuries and 32% of deaths [2] [3]. One study that focused on a light reconnaissance battalion found that 97% of injuries and deaths in that group were caused by explosives with 65% from IEDs and 32% from mines [4]. An obvious way to increase the protective capabilities of armored vehicles is to increase the thickness of the armored hull. However, today's vehicles are approaching mass limits beyond which they will not be compatible with road surfaces or other terrain encountered in theatre. Further, while these vehicles are effective at shielding the occupants from the overpressure caused by the blast shock waves, the high acceleration of the vehicle in response to momentum transfer from explosive shock and soil ejecta can cause severe injuries. A particular concern comes from IEDs detonated directly below the vehicle. Particular studies on injuries caused by IEDs show that violent acceleration of the floor and seats primarily cause irreparable damage to the soldier's feet, legs, spine, and head [3]. Steps have been taken to reduce the transmission between the outer hull of the vehicle and the troop compartment floor, and additional measures are continually being examined and evaluated.

Along with injuries to the legs and spine, as many as 20% of casualties in Iraq were diagnosed with traumatic brain injury TBI [5]. These brain injuries are often life-altering and not always readily apparent in that they may take weeks to manifest observable symptoms. While V-shaped hulls are implemented in order to mitigate blasts from below the vehicle and ever-improving armored plating is used to protect against projectile and explosive hull penetration, other measures should also be considered to improve even

further the force protection levels to counter current and future threats [6].

DUAL-HULL DESIGN AND OPTIMIZATION

Acceleration in response to blasts originating from the bottom and side of Mine-Resistant Ambush-Protected (MRAP) vehicles must be lessened if there is to be any useful change to protect the vehicle's occupants. To accomplish this, a dual V-hull arrangement, with energy absorbing structure separating the two hulls, is proposed. Through a constrained optimization approach, the mass distribution, spring constants, and damping characteristics of this blast attenuation system can be systematically adjusted to minimize occupant acceleration, thereby preventing or reducing potential traumatic injuries, while still remaining within realistic materials and mass limitations.

The first problem in approaching the situation lies in the complexity of the overall system, arising from the geometry of the vehicle and the dynamics of the human body in response to high amplitude, short duration acceleration. In the face of this complexity, the feasibility of the countermeasure concept and the value ranges for system design parameters can be conveniently examined by approximating the outer hull, the inner hull, and the human in their seat as a three lumped-mass system (see Figure 1). These masses are connected through a simple set of spring-damper couplings used for shock absorption.

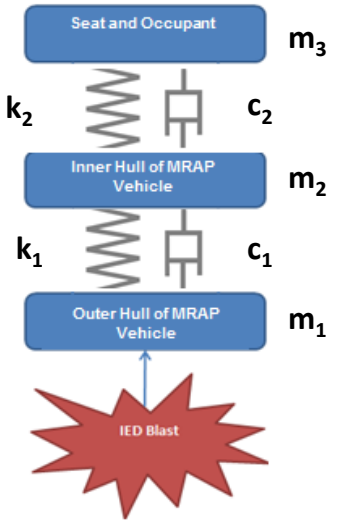

Figure 1: Lumped-mass model of the proposed blast mitigation system

After the simple lumped-mass model has been optimized, the next step is to develop and utilize a more detailed finite element model using realistic vehicle and human occupant geometries and material properties. The blast event itself is modeled through smoothed particle hydrodynamic (SPH) representation of the explosive charge and soil which interacts with the finite element vehicle structure through contact modeling methods.

Optimization of Lumped-Mass Model

There are several options available when optimizing the equations of motion of this system. First and foremost, one must identify the parameter that must be minimized or maximized. In this case, it is the peak acceleration of the occupant over the simulation time (0.1 seconds) that will be minimized. As shown by Equations 1-3, there are many parameters to consider, including two spring constants (k_1, k_2), two damper constants (c_1, c_2), and three masses (m_1, m_2, m_3). Allowing nearly all of these values to change creates a very challenging optimization problem. It should also be noted that the blast in this case is being treated as a blast force (F) equally distributed over the entire bottom hull and acting strictly vertically, while later a more sophisticated method will be utilized in simulating the blast loading on the vehicle.

$$m_2\ddot{q}_1 + c_1\dot{q}_1 + k_1q_1 - c_1\dot{q}_2 - k_1q_2 = F \quad (1)$$

$$m_2\ddot{q}_2 + c_1\dot{q}_2 + c_2\dot{q}_2 + k_1q_2 + k_2q_2 - c_1\dot{q}_1 - c_2\dot{q}_3 - k_1q_1 - k_2q_3 = 0 \quad (2)$$

$$m_3\ddot{q}_3 + c_2\dot{q}_3 + k_2q_3 - c_2\dot{q}_2 - k_2q_2 = 0 \quad (3)$$

The topmost equation (1) represents the response of the outer hull, the middle equation (2) gives the response of the inner hull, and the last equation (3) gives the response of the occupant of the vehicle. The q values are the displacement, velocity, and acceleration of each mass.

The most significant challenge in the simulation is runtime. In a situation with fewer constants to operate with, say one or two constants, one would be able to run a brute force optimization method. That is, one could simply change a constant by a small value and run the simulation and repeat until that constant is optimized for the smallest peak acceleration over the timeframe. However, as more constants are introduced, due to the way multiple constants are used in multiple equations of motion, every possible combination must be explored, which can become excessively time consuming.

In this case, using a basic MATLAB code, the desired simulation (0-0.1 seconds) can be run roughly 10 times in one second. For the sake of simplicity, for this theoretical situation, only the spring and damping constants are optimized, while the masses will stay the same. If one was to run the simulation for just 10 different values for each of these constants, making incremental adjustments, a total of 10,000 simulations must be run in order to explore every possibility and obtain a true minimum peak acceleration in this data set. This minimal calculation takes 975 seconds or roughly 16 minutes on a standard lab computer in the Engineering Research Center at the University of Cincinnati. Expanding the search space to explore a range of 100 different values for each of the constants and the total run time grows to approximately 10 million seconds or roughly 116 days. Such long runtimes for such a simple model are unacceptable and an alternative approach had to be pursued.

When starting the optimization, nearly every variable in the simplified system is subject to modification during a manual heuristic-based optimization: all 3 masses, both springs, both dampers, and the distance between the three

masses. Once a reasonable baseline for the variables is set, the system is subjected to the appropriate force needed to simulate a roadside IED (a 5 millisecond explosion reaching a peak 217 Gs or 2128.04 Newtons force per kilogram) [7] and the optimization problem begins.

The final step in the simple simulation is mathematical optimization, where a cost-function is formed to take into account a number of the system outputs. The acceleration of the occupant is the primary variable in need of minimization, but as a whole, the cost function includes:

- Peak Acceleration of the Occupant
- Total Impulse
- Acceleration of the Occupant's Head
- Spinal Compression of Occupant

The constraints include:

- Mass of hull
- Mass of cabin
- Mass of occupant/seat
- Distance between masses
- Coefficient of springs
- Coefficient of dampers
- Realistic spring-damper values

Other constraints not considered in this analysis include vehicle geometry (road width, bridge height) and soldier body and personal protective equipment masses.

The optimization method used in this study was from the class of optimizations called 'reduced gradient' or 'gradient projection'. These are methods that extend linear constraints to work for non-linear constraints, which is needed for the situations examined in this study. The procedure begins with a non-linear optimization problem expressed with equality constraints as follows:

$$\text{Optimize: } y(\mathbf{x})$$

$$\text{Subject to: } f_i(\mathbf{x}) = 0 \qquad \text{for } i = 1, 2, \ldots, m$$

where m is equal to the number of constraint equations and there are n independent variables. By converting the constrained problem into an unconstrained problem, the Generalized Reduced Gradient (GRG) method uses direct substitution to reduce the number of independent variables to n-m and eliminate some constraint equations. With nonlinear constraint equations, though, it is not feasible to solve the remaining n-m variables and substitute into an economic model. As such, we can turn to constrained variation and Lagrange multipliers to seek minima and maxima in this nonlinear case. In the economic model, a Taylor series is expanded but only the first order is retained to use with the constraint equations to once again reduce the number of independent variables.

A simple generic case containing two independent variables and a single constraint equation is a convenient way to demonstrate this concept:

$$\text{Optimize : } y(x_1,x_2)$$

$$\text{Subject to: } f(x_1,x_2) = 0$$

Expanded in a Taylor series about $x_k(x_{1k},x_{2k})$ gives:

$$y(\mathbf{x}) = y(\mathbf{x_k}) + \frac{\partial y}{\partial x_1}(\mathbf{x_k})(x_1 - x_{1k}) + \frac{\partial y}{\partial x_2}(\mathbf{x_k})(x_2 - x_{2k}) \tag{5}$$

$$0 = f(\mathbf{x_k}) + \frac{\partial f}{\partial x_1}(\mathbf{x_k})(x_1 - x_{1k}) + \frac{\partial f}{\partial x_2}(\mathbf{x_k})(x_2 - x_{2k}) \tag{6}$$

And further substitution of Equation 6 into Equation 5 to eliminate x_2 gives:

$$y(\mathbf{x}) = y(\mathbf{x_k}) - \left(\frac{\partial y}{\partial x_2}(\mathbf{x_k})\right)\left(\frac{\partial f}{\partial x_2}(\mathbf{x_k})\right)^{-1} f(\mathbf{x_k})$$

$$+\left(\frac{\partial f}{\partial x_2}(\mathbf{x_k})\right)^{-1}\left[\frac{\partial y}{\partial x_1}(\mathbf{x_k})\frac{\partial f}{\partial x_2}(\mathbf{x_k}) - \frac{\partial y}{\partial x_2}(\mathbf{x_k})\frac{\partial f}{\partial x_1}(\mathbf{x_k})\right](x_1 - x_{1k}) \tag{7}$$

The first two terms given in the above equation are known constants being evaluated at point x_k. The coefficient of x_1-x_{1k} is also known and gives x_1 the cue to move in the positive or negative direction. To compute the stationary point, one must define $dy/dx_1 = 0$, and the result is the same as for the equation given in the square brackets in the above equation, the constrained variation. The terms in the brackets can be seen as giving the direction to move away from x_k to find improved values of the economic model and fulfill the constraint equation. This is only a brief discussion of the Generalized Reduced Gradient method. A more detailed explanation can be found in the text by Pike [8].

Having selected the GRG method as the means to optimize the response of the vehicle in our three-mass system, the next step was to apply this method to the equations of motion presented in Equations 1-3.

The GRG solution was performed in Excel (Microsoft Corporation, Redmond, WA). Equations 1-3 were solved over time to determine the accelerations of the outer hull, inner hull, and occupant. Using the initial conditions of velocity and distance for the masses, the acceleration was numerically integrated to determine the velocity and displacement over the time course of interest.

After the time-response was determined, the next step was to employ the Generalized Reduced Gradient optimization process. The peak acceleration of the occupant was selected as the parameter for minimization. The variables that the solver could modify in order to minimize the target were k_1, k_2, c_1, c_2, m_1, and m_2. Next, the constraints were applied, namely:

- c_1, c_2, k_2, m_1 and m_2 must be greater than or equal to 1 to be physically realistic
- The total mass (m1+m2) is held equal to 6803 kg to maintain vehicle performance

This final constraint was to ensure that the masses must never cross paths, since in real life the outer hull would never overtake the inner hull or the occupant.

During the initial iterations using the GRG Solver, the values for the constants were modified by hand and the results of each situation were logged. In these cases c_3 was made equal to c_1+c_2 and k_3 equals k_1+k_2, where c_3 and k_3 were metrics added to make calculation of the mass response easier. At this time, k_1 was fixed so that the outer hull and inner hull system would stay stiff enough for the hulls to remain at 10 cm apart during vehicle gravity loading alone.

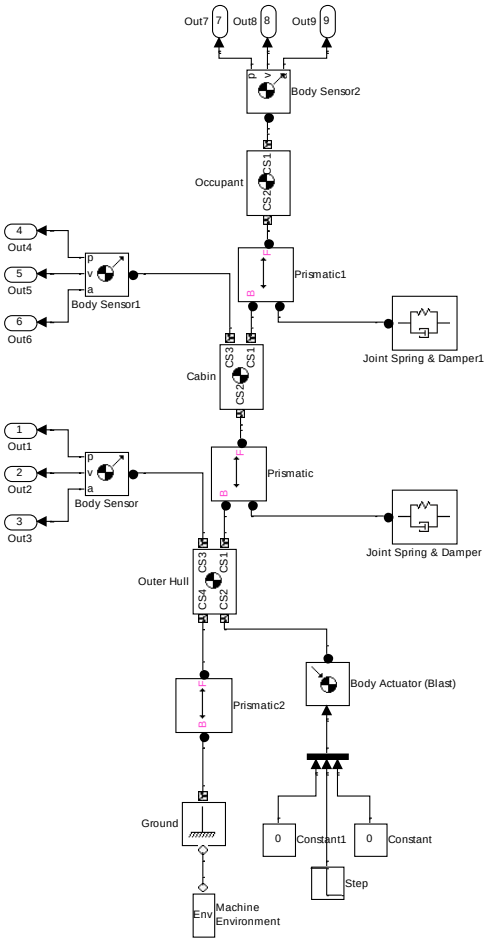

Figure 2: SIMMECHANICS model of three-mass representation of dual-hull and occupant.

Lumped-Mass Model Verification

While the lumped-mass model could not be experimentally validated to this point, a model verification was performed by comparing the results of the Excel-based simulation to a MATLAB SIMMECHANICS model (see Figure 2). The results matched identically.

Dual-Hull Proof-of-Concept Model

To determine if the dual-hull concept appropriately reduces both hull deformation and total kinetic energy imparted to the hull, a test was created using the DRDC plate model described in a previous conference manuscript [9]. The quarter-symmetric model included a single metal plate mounted on a frame with soil SPH particles placed below the plate and a SPH TNT-charge placed within the soil. The explosive charge and soil model were previously validated through comparison with the DRDC plate test [9]. In this study, a standoff plate (outer hull) was placed 10 cm below the original plate and a line of spring-damper elements were created to connect the two plates with the purpose of mitigating both displacement and energy transferred to the upper plate. Figure 3 shows the new configuration, where the green vertical 1-D elements represent the combined spring-damper elements.

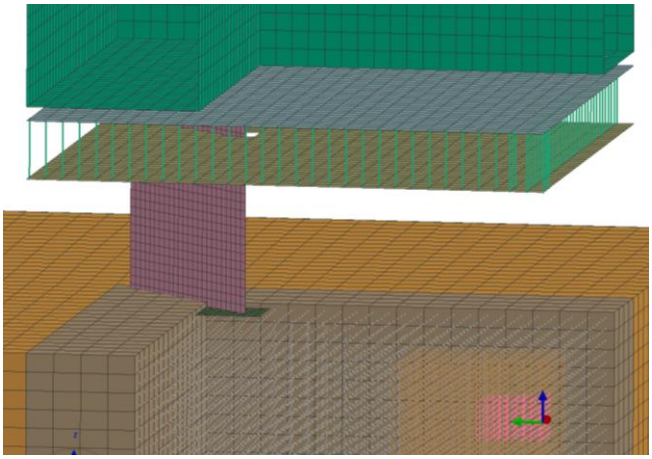

Figure 3: Proof-of-concept simulation using modified DRDC plate model.

Dual-Hull High-Fidelity Simulation with Generic Hull Model and SPH Blast Modeling Proof-of-Concept

Historically, the Department of Army has had difficulty collaborating with industry and academia on underbody blast events due to the sensitive nature of the work. Data generated from testing military vehicles is typically rated CLASSIFIED and not readily sharable. To alleviate this issue, the Army Research, Development and Engineering Command-Tank Automotive Research, Development and Engineering Center (RDECOM-TARDEC) has fabricated a

generic vehicle hull (Figure 4) with the intent to share data with academia and the industry to spur innovation in blast mitigation technologies [9, 10]. For this study, a high-fidelity representation of the dual-hull system in combination with the TARDEC Generic Hull model was developed. In order to analyze and optimize the performance of the proposed blast mitigation system, several modifications were made to the existing generic hull blast model. Firstly, a second layer of hull was added beneath the existing hull at a standoff distance of 10 cm below the original hull. A set of spring-damper elements were connected between the hulls to provide shock absorption and energy dissipation, as shown in Figure 5.

Figure 4: Generic Hull Test Vehicle.

Several spring-damper distribution patterns were attempted via a trial-and-error process. The GRG optimization method described earlier was used to determine the stiffness and damping constants for these distributed interface elements. The vehicle weight distribution between the hulls was also adjusted during the optimization. Another set of spring-damper elements was placed between the occupant's seat and the inner hull to represent the energy absorption feature of the occupant seat (Figure 6). This is in contrast to the original Generic Hull model in which the seat is mounted on the side of the hull with a rigid connection.

The dummy model utilized in the simulations provided access to a standardized set of human injury metrics. These included head acceleration, neck tension and compression, chest acceleration, and femur load.

RESULTS

Lumped-Mass Model Optimization

Figure 7 provides a visual representation of the iterations using the combination of the GRG Solver and hand calculations to come up with an adequate minimization for this set of equations. One can see that, with a proper

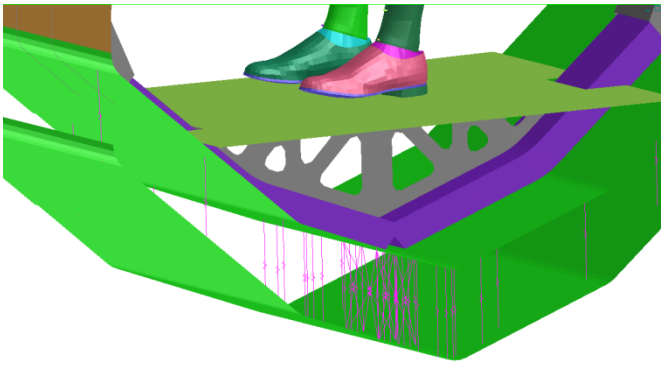

Figure 5: The spring-damper element setup between the outer hull and inner hull as viewed in the portion of the hull directly below the occupant .

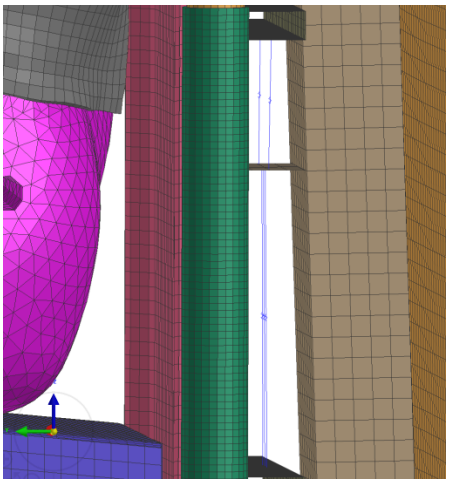

Figure 6: The spring-damper element configuration between the inner hull and the occupant's seat. This is the final configuration where 5 elements are used.

understanding of the effects springs and dampers can have on the resulting acceleration, it is possible to reduce the acceleration of the occupant from 21.7 Gs to a low of 1.48 Gs.

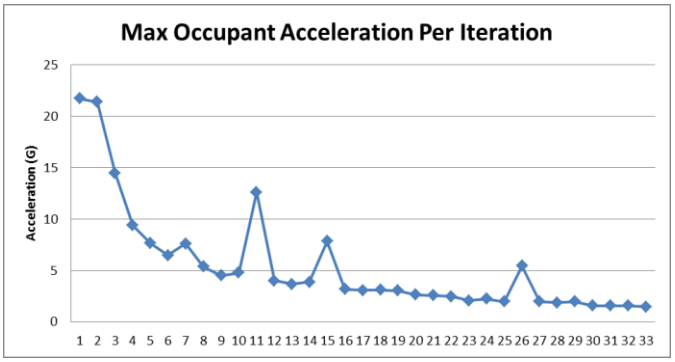

Figure 7: The maximum acceleration of the occupant in the lump-mass exploration using handpicked values. Each number on the x-axis stands for an iteration.

After the optimization exploration was complete, the next step was to run the GRG Solver to refine the estimates and obtain a formal optimum solution. Table 1 shows the final solution, with the optimized coefficients and the final acceleration of the occupant: "MAX ABS Q3DD", as given in Gs.

Figures 8, 9 and 10 display the most important responses of the lump-mass simulation, namely, the acceleration of the outer hull subject to the blast pulse, the acceleration of the occupant, and the displacement of all three masses relative to each other. Only the first 0.035 seconds are displayed

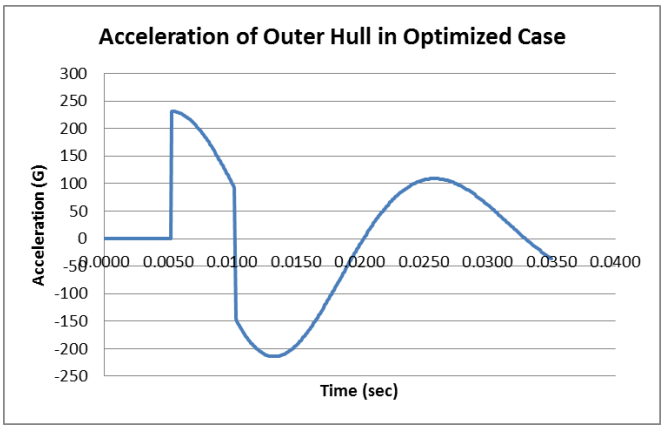

Figure 8: The acceleration response of the outer hull over time in the GRG optimized case. The first 5 milliseconds represent the pre-blast time, while the next 5 milliseconds represent the blast.

because all the relevant peaks are contained in this window. As seen in the acceleration figures, the first 0.005 seconds display the pre-blast time. During this time, the occupant and inner hull remain upright and stable indicating that the initial preload applied to the springs accurately represents the amount of preload that would occur due to gravity settling. After the initial blast force, which lasts from 0.005 seconds to 0.01 seconds, one sees the acceleration of the

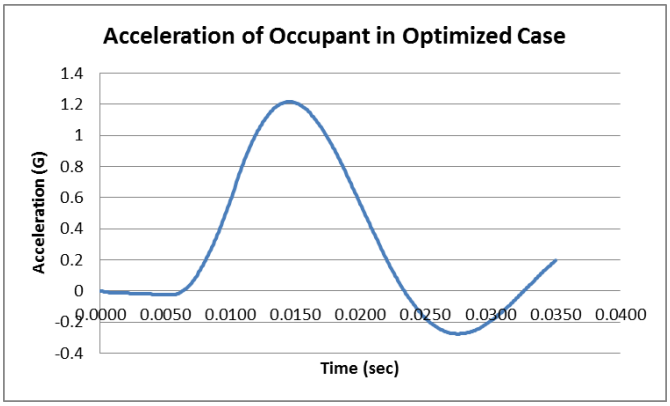

Figure 9: The acceleration response of the occupant over time in the GRG optimized case.

outer hull switch immediately to negative G's and reach a local minimum just before 0.015 seconds. This rebound effect can be explained by the spring with a rate of 500,000

Table 1: The best case scenario for the optimized lumped-mass simulation utilizing the GRG Solver.

c1	c2	c3	k1	k2	k3
36933	250	37183	500000	15731	515731

m1	m2	m3		Preload?	F
6425	378	82.6		0.005 secs	14677221

MAX ABS Q3DD
1.215

N/m pushing back on the outer hull after the blast force is no longer applied. Very soon after the blast, the momentum is transferred through to the occupant, which reaches its absolute maximum acceleration of 1.215 Gs at 0.0143

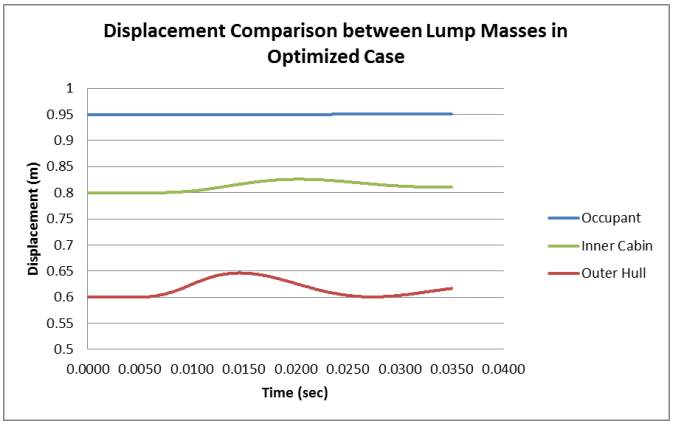

Figure 10: A comparison of the occupant, inner hull, and outer hull's displacement over time for the best-case lump-sum blast mitigation system using the GRG Solver.

seconds. The displacement plot of Figure 10 shows the response of the three masses and one should note the occupant barely moves within the initial 0.035 seconds in this highly idealized case.

Dual-Hull Proof-of-Concept with DRDC plate

The DRDC plate test simulation was run with and without the dual-hull blast mitigation system in place. The effectiveness of the blast mitigation system is dependent on the displacement and energy imparted to the plate. Figure 11 compares the displacement of the upper plate at the final time step. The original test result (without the added plate) is shown on the right. The final displacement with the spring-damper system in place is shown on the left. The left side experiences a substantial decrease in displacement as a whole. Also, at the final time step, the plate in original system receives 605.1 kJ of energy from the blast, while the upper plate in the mitigated system receives 57.1 kJ of transmitted energy. The difference in magnitude of both metrics provided strong indication that the dual-hull concept would reduce vehicle and occupant acceleration in the full-scale model.

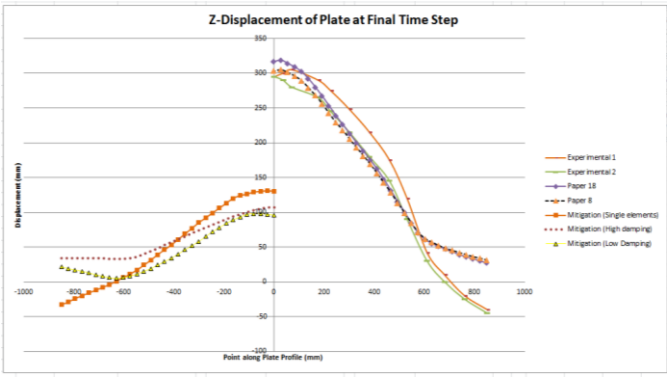

Figure 11: Result of the DRDC plate proof-of-concept. On the left is the displacement of the plate with blast mitigation, on the right is the displacement without the system in place.

Dual-Hull Optimization

A substantial portion of the time spent optimizing the dual-hull system was dedicated to a manual search for an appropriate type and distribution of spring-damper elements. This sequence is depicted in Figure 12. In runs 1 through 14, the distribution of elements was changed from a central concentration along the keel midline to full coverage of the v-hull surface. For run 15, the connecting elements were changed from bar elements to 6-DOF spring-damper elements. By run 26, a truss arrangement had been formed to stabilize the hull displacement in response to non-symmetric blast loading.

Occupant Response in Generic Hull Model

Figure 13 provides a visualization of the dummy's response to the blast under the baseline case (single hull, left side of figure) and the best case with the dual-hull system in place (right side of figure). It is visually evident that the baseline case provides a noticeably more violent reaction than the best case dual-hull scenario. The best case sees the dummy depress into the seat, and the feet are pushed against the floor, but without a violent rebound. The baseline, without the dual-hull blast mitigation feature, causes the dummy to be violently launched into the air due to the impact of the blast transferred through the inner hull, seat, and floor.

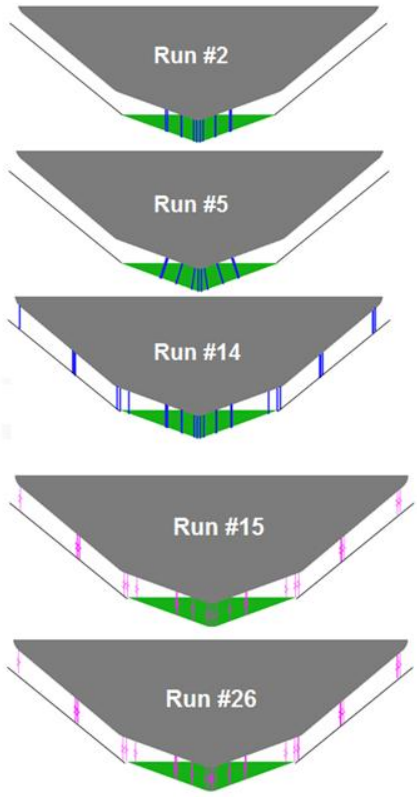

Figure 12: The evolution of spring configurations as simulations progressed. The iterations are, from the top to the bottom: Run 2, 5, 14, 15, and 26.

Figure 13: Occupant (ATD) response to blast in baseline case (left column) versus dual-hull (right column) at time points (from top to bottom) of 24 ms, 50 ms, 74 ms, and 100 ms.

Figure 14 shows the acceleration of the human dummy's head over the length of the simulation for selected iterations, including the baseline run. The top chart shows the baseline run, best case, and two intermediate cases involving significant improvements in the blast mitigation system design, such as new spring configurations and hull weight distributions that led to decreases in occupant acceleration. The lower chart shows only the baseline and best case (iteration 26) to visually demonstrate the dramatic improvement in blast mitigation.

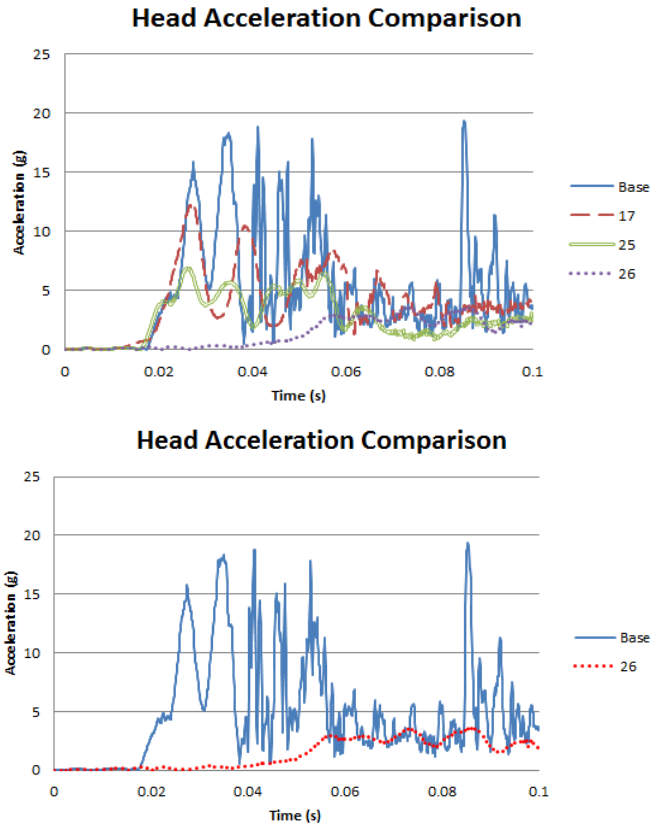

Figure 14: Comparison of head acceleration for baseline and simulations 17, 25, and 26 (top), and baseline and simulation 26 only (bottom).

Figure 15 shows summary plots of head acceleration, neck compression, chest acceleration, and left femur load for all of the simulation runs, the first bar, labeled "Base" and colored grey, represents the baseline blast without any blast mitigation features. Conversely, the green bar labeled "26" represents the best blast-mitigation case to come out of this optimization process. There is a general trend toward a less violent response with successive iterations, showing the success of the combined heuristic and mathematical optimization approach. A full table of the numerical results for each injury criterion (head, neck, chest, legs) for all simulations can be found in Appendix A.

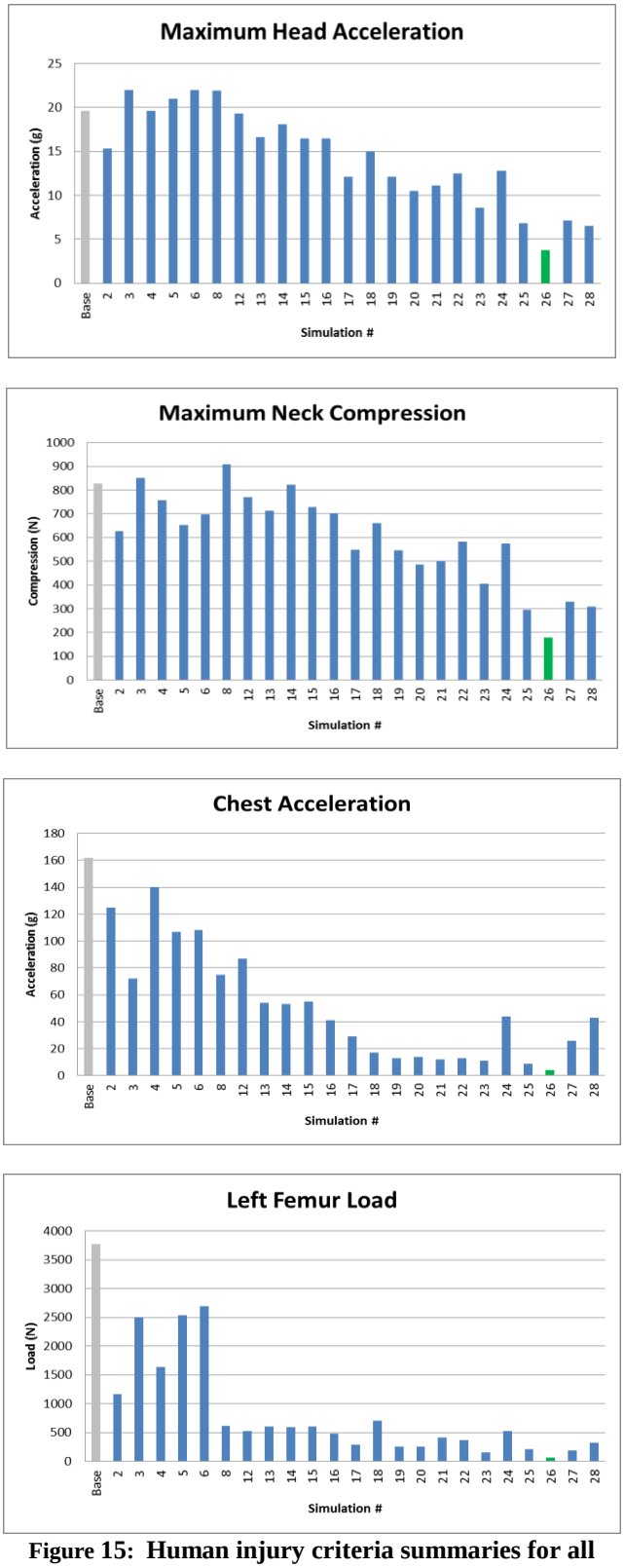

Figure 15: Human injury criteria summaries for all simulation runs. The baseline (first column) is displayed in grey, while the best case (# 26) is shown in green.

Figure 16 provides a comparison of the calculated Head Injury Criteria (HIC) values for selected key simulations. While the baseline case produces a HIC of 1690 and case 17 produces a HIC of 995, the later iterations 25, 26, and 28 have HIC ratings of 381, 72, and 424, respectively.

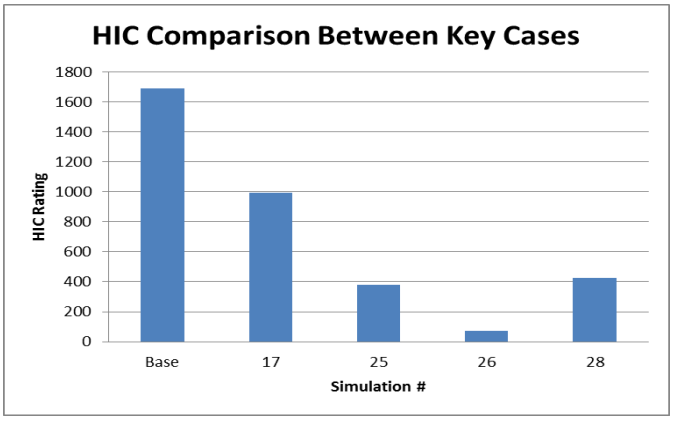

Figure 16: A comparison of the Head Injury Criteria for key simulations of the blast mitigation system, including the baseline case and the best case (26).

DISCUSSION

The lumped-mass model provided an expedient coarse adjustment process for the dual-hull system parameters prior to commencing the time-consuming full-vehicle simulations. At the same time, the lumped-mass model facilitated the use of the Generalized Reduced Gradient method of optimization.

The ultimate measure of the effectiveness of the blast mitigation system comes from the human injury criteria. In the baseline case, the Head Injury Criteria was calculated to be 1690, which is more than double the HIC limit of 700 that represents a high risk of brain injury. As such, this metric plays a valuable role in assessing the effectiveness of the proposed blast mitigation system. The first set of attempts at blast mitigation (through run 12) actually worsened the effect and created higher head accelerations for the occupant. At first it was thought that the number of springs and the coverage they provided created an adverse effect. The initial layout of 16 spring-damper elements was changed to a layout consisting of 98 total spring-damper elements. While the 98 spring-damper configuration was implemented by Run 6, the HIC results did not show improvement in Run 6 through Run 12. Up through Run 12, the blast mitigation system was using a set of 1-dimensional bar elements with the option to take on spring and damper coefficients. The HIC and other injury criteria results began to improve when the bar elements were replaced with 6-DOF spring-damper elements in Run 13. This change initially produced a small decrease in head acceleration, but it was still above the injury threshold, so more changes were needed.

Runs 14 through 24 experimented with different types of spring-damper configurations and slight modifications of the spring and damping coefficients. It appeared that not all of the spring-damper elements were being engaged fully. Furthermore, none of these responses were performing in a way that moved the HIC to a safe range. For example, the HIC in Run 17 was 995, still well above the injury threshold. The breakthrough in reducing the HIC value came in the way the weight was distributed in the vehicle. In all the simulations up through run 24, the changes in weight distribution were managed through changing the density of the materials, meaning the armor was heavier in the outer hull but no thicker than normal. In run 25, the material was changed back to the density of normal steel plating and instead, the weight was increased by increasing the thickness of the shell. As such, the weight remained in the proper distribution calculated in the lumped-mass optimization section, but the thicker plating caused the simulation to show both more realistic and more promising results. This is because the plate thickness changes appropriately accounted for the increasing stiffness of the outer hull.

There is a tradeoff inherent in the mass distribution changes. As the outer hull becomes thicker and stiffer, and the inner hull becomes thinner and less stiff, there will be a point at which the inner hull can no longer sustain the loads transferred through the intermediary structure connecting the inner hull to the outer hull. This tradeoff will be examined in follow-up studies.

In run 25, the HIC finally dropped significantly to a value of 381, well below the injury threshold. However, the system must account for varying blast strength and varying placement relative to the hull, so further improvement in the robustness of the system was desirable. The configuration simulated in Run 26 brought together the lessons learned to that point by creating a blast mitigation system with full-hull coverage, optimal spring-damper constants, and the correct means of mass distribution. The HIC value of 72 seen in run 26 is a dramatic improvement over the baseline case. Runs 27 and 28 were not used to improve on run 26, but to confirm that the correct inner-hull-to-occupant-seat connection was being used in run 26.

The head is only one of many major areas of concern when it comes to explosive acceleration and the rest of the body must be examined for injury as well. Since the neck compression never exceeds a maximum of 828 N for all simulation runs, including the baseline case, and since this is well below the NHTSA threshold of 5440 N this is not an area of concern. Nevertheless, it is interesting to note that the neck compression was reduced to as low as 180 N for the best case, run 26, thus providing further evidence of the effectiveness of the blast mitigation system.

The maximum chest acceleration of 162 Gs, observed for the baseline case, exceeded the NHTSA maximum allowable value of 55 Gs by a substantial margin. Clearly there was a need for improvement here. As the runs progressed, values for this criterion were progressively decreased, reaching a value of 108 Gs when the full-coverage spring-damper system was implemented. The value dropped further, to around 55 Gs, when the spring-damper element type change was introduced. The biggest change, once again, came when the weight distribution between the hulls was adjusted through wall thickness changes. In Case 26, the maximum chest acceleration was reduced to a low of 4.1 Gs, an order of magnitude under the injury threshold and a dramatic improvement over the baseline case.

The final injury criterion considered was femur load. While both the left and right femur loads are given in the injury reports generated by the simulation, the left leg constantly underwent higher loads due to the positioning of the dummy. The femur load of 3771 N for the baseline case was well below the 9074 N injury threshold, so this injury type was not a concern. Still, as the runs progressed, the best case once again emerged in run 26, where the maximum femur load was reduced to 61 N. Again, this is a major improvement over the baseline case, providing further confirmation that the mitigation scheme is successful in this idealized simulation scenario.

While the results of this dual-hull approach appear extremely effective for blast mitigation and increasing occupant safety, a few factors must be kept in mind. This research, while done with the use of the TARDEC generic hull model, was not accomplished with any of the operational constraints of the vehicle in mind other than simple mass distribution and hull displacement limitations in order to maintain a base level of vehicle functionality. However, the mass distribution constraint in this study does not address at any depth how the vehicle's performance on the battlefield is affected by using lighter materials for the side, roof, and floor paneling or having a majority of the weight distributed to the lower hull. As such, further work should address acceptable safety and performance parameters for armored vehicles.

Another factor that must be investigated to determine the feasibility of this system comes in the form of the spring-damper system between the outer and inner hulls. A realistic interface needs to be designed and verified through simulation before an experimental prototype can be fabricated. While this interface may take the form of a collapsible honeycomb structure, a distributed set of small springs and dampers, magnetorheological fluid, or some other means, it is possible that there may be no physical materials available that can provide the stiffness and damping properties that are suggested by the best-case results in this numerical simulation study. The real-world material and geometric properties of a physical system will greatly factor into the effectiveness of an actual dual-hull system.

In the event of further work, the influence of directional and offset blasts also warrants exploration. While the dual-hull system appears to be very effective at attenuating blasts originating directly beneath the vehicle, it is not clear how the system would perform for blasts detonated further towards the front, back, or sides of the vehicle. Also, redistributing weight to the outer hull may limit the weight, and consequently thickness and effectiveness, of the armor on the sides and other portions of the vehicle and this compromise will have to be considered.

It would be sensible to perform a few long time-duration simulations of the best case dual-hull system. In the lumped-mass system, the outer hull saw considerable spring-back after the initial acceleration, but in the finite element simulation, no such rebound occurred. As such, a simulation that runs out to 0.5 seconds or 1 second could be useful in determining if there would be adverse reactions from the system aside from the initial blast absorption.

Another needed improvement is to initiate the simulation with more realistic contact between the occupant and the seat and floor. This would be done by first performing a gravity-settling simulation run to allow the human/ATD model to compress the seat cushioning and rest its feet on the floor. Seat compression and spine alignment could have profound influence on the human injury criteria results.

Finally, the human dummy model in this simulation was not restrained by seat belts. Future simulations will need to include restraints in order to improve realism.

CONCLUSIONS

The simulations conducted in this exploratory effort indicate that the dual-hull system has a great deal of promise for mitigating blast-induced occupant acceleration and loading. Further work should focus on enhancing the realism of the vehicle configuration and better accounting for operational constraints such as reduced ground clearance.

An attractive feature of the design is that it could be developed as an add-on countermeasure that would not require extensive modification to existing vehicles and could be designed to avoid interfering with other countermeasure systems. However, even as an add-on system, the loads transferred between the outer hull and the inner hull will be concentrated at certain locations. The effect of this type of interface would clearly need to be considered during the design stage, and evaluated through simulation and live-fire testing.

REFERENCES

[1] Wilson, "Improvised Explosive Devices (IEDs) in Iraq and Afghanistan: Effects and Countermeasures," *CRS Report for Congress*, August 2007, pp. 1-6.

[2] Kasulke, RJ: Army Medicine: Advances in Combat Casualty Care. AMSUS-SM Meeting, 2009.

[3] Ramasamy A, Harrison SE, Clasper JC, Stewart MPM: Injuries From Roadside Improvised Explosive Devices. J Trauma, 2008; 65(4): 910-914.

[4] Gondusky JS, Reiter MP: Protecting Military Convoys in Iraq: An Examination of Battle Injuries Sustained by a Mechanized Battalion During Operation Iraqi Freedom II. Military Medicine, 2005; 170: 546-549.

[5] Hartings JA, Totella FC, Strong AJ, Bhatia R, Bullock MR, Fabricius M, Vo AH, Bell RS, Armonda RA, Ecklund JM, Dreier JP: Spreading Depolarizations of Cerebral Cortex After brain Injury: Mechanism of Injury Progression and Relevance to Military Neurotrauma. Walter Reed Army Institute of Research, 2006.

[6] Military Factory, "Buffalo H Mine Resistant Ambush Protected Vehicle (MRAP) Multi-Purpose Armored Vehicle," www.militaryfactory.com, July 2010.

[7] Nilakantian, Tabiei, "Computational Assessment of Occupant Injury Caused by Mine Blasts underneath Infantry Vehicles," *International Journal of Vehicle Structures & Systems*, 2009, Volume: 1, pp. 50–57.

[8] Pike R, "Multivariable Optimization Procedures", Optimization of Engineering Systems, Louisiana State University, November 2001.

[9] Dooge D, Dwarampudi R, Schaffner G, Miller A, Thyagarajan R, Vunnam M, Babu V, "Evolution of Occupant Survivability Simulation Framework Using Fem-Sph Coupling," NDIA Ground Vehicle Systems Engineering And Technology Symposium, Modeling & Simulation, Testing And Validation (MSTV) Mini-Symposium, Dearborn, Michigan, August 9-11, 2011.

[10] R. Scherer, "Vehicle and Crash-Dummy Response to an Underbelly Blast Event", 54th Stapp Conference (Oral Only).

Appendix A

The table below shows human injury criteria results for all generic hull simulation runs.

Run #	Max Head Acceleration (G)	Neck Tension (N)	Neck Compression (N)
Base	19.6	401	828
2	15.3	311	626
3	22	280	850
4	19.6	352	758
5	21	274	652
6	22	342	697
8	21.9	280	907
12	19.3	344	769
13	16.6	388	713
14	18.1	354	821
15	16.5	278	728
16	16.5	303	702
17	12.1	250	548
18	15	4.4	660
19	12.1	4.3	547
20	10.5	4.5	486
21	11.1	4.4	503
22	12.5	4.4	582
23	8.6	4.6	406
24	12.8	259	576
25	6.8	230	295
26	3.8	10	180
27	7.1	191	329
28	6.5	137	309

Run #	Chest Acceleration (G)	Left Femur Load (N)	Right Femur Load (N)
Base	162	3771	1908
2	125	1162	1640
3	72	2500	900
4	140	1633	980
5	107	2538	954
6	108	2692	1010
8	75	617	404
12	87	527	398
13	54	599	411
14	53	590	438
15	55	602	375
16	41	480	287
17	29	291	299
18	17	700	804
19	13	261	222
20	14	252	128
21	12	417	359
22	13	367	211
23	11	160	116
24	44	530	352
25	8.7	209	134
26	4.1	61	68
27	26	193	136
28	43	328	156